JOURNAL OF QUATERNARY SCIENCE (2011) **26**(1) 109–117 ISSN 0267-8179. DOI: 10.1002/jqs.1438

High-resolution X-ray fluorescence core scanning analysis of Les Echets (France) sedimentary sequence: new insights from chemical proxies

MALIN E. KYLANDER,[1]* LINDA AMPEL,[1] BARBARA WOHLFARTH[1] and DANIEL VERES[2]
[1]Department of Geological Sciences, Stockholm University, SE 10961 Stockholm, Sweden
[2]Emil Racovita Speleological Institute, Cluj, Romania

Received 4 February 2010; Revised 30 June 2010; Accepted 8 July 2010

ABSTRACT: The Les Echets sediment sequence has recently been the subject of a high-resolution, multi-proxy study which revealed shifts in lake productivity linked to Greenland stadials and interstadials over the last 40 ka (Wohlfarth *et al.*, 2008. Rapid ecosystem response to abrupt climate changes during the last glacial period in western Europe, 40–16 ka. *Geology* **36**: 407–410). Here we present new elemental data for this sequence as acquired using an X-ray fluorescence core scanning system which provides *in situ* high-resolution, continuous, multi-element analyses. It was found that the strength of associations between the studied elements (Ti, Rb, K, Zr, Si, Ca, Sr, Mn and Fe) varied over time with changes in lake status which are ultimately driven by changes in climate. Increases in fine-grained, detrital input (as indicated by Ti, Rb, K and Zr/Rb) overlap with independently established periods of lower lake productivity and are interpreted to represent more arid conditions. Several of these arid periods are coincident with low diatom concentrations and the timing of Heinrich events H4, H3 and H2. The duration of the environmental impacts linked to the H events varied by proxy with elemental data (Ti and Zr/Rb) estimating shorter events than the diatom data. Periods of lower detrital input and coarser grain sizes agreed in time with periods of higher lake productivity. The elemental data provide new insights into hydrological changes and related sediment processes within the catchment, and highlight the need for multi-element and multi-proxy approaches when reconstructing climate change using lacustrine sediment sequences. Copyright © 2011 John Wiley & Sons, Ltd.

KEYWORDS: XRF core scanner; lake sediment; Heinrich event; elemental chemistry; palaeoproxy.

Introduction

The climate of the Last Glacial (ca. 115–11.5 ka), was characterised by dramatic changes and significant contrasts ranging from very cold and harsh to more temperate conditions. The Last Glacial Maximum (LGM) occurred between 26.5 and 19 ka and had a substantial influence on environments worldwide (e.g. Clark *et al.*, 2009). Even though this period corresponded to the maximum ice extent, the most severe climatic coolings (at least in the mid latitudes in the Northern Hemisphere) were associated with six distinct periods referred to as Heinrich (H) events which occured between ca. 65 and 15 ka (de Abreu *et al.*, 2003; Roucoux *et al.*, 2005; Fletcher and Sánchez Goñi, 2008; Sánchez Goñi *et al.*, 2008). In addition, rapid oscillations between cold stadials and warm interstadials, referred to as Dansgaard–Oeschger (DO) cycles are found more or less throughout the Last Glacial but were most frequent between ca. 60 and 25 ka (Johnsen *et al.*, 1992; Dansgaard *et al.*, 1993). These oscillations are now conventionally referred to as Greenland stadials and interstadials (Lowe *et al.*, 2008). Comparisons between marine sediment cores and Greenland ice cores have shown that H events typically took place during a stadial phase at the end of a series of stadial–interstadial cycles that became progressively colder (Bond *et al.*, 1993). The origin of these rapid and dramatic shifts in climate that occurred before and after the LGM and their impact on the landscape and environment in different regions have been important questions in palaeoenvironmental studies during the last two decades.

In Europe, environmental changes throughout the Last Glacial have been reconstructed at several sites including Les Echets, a former lake basin in eastern France (de Beaulieu and Reille, 1984). The sediments from Les Echets have recently been the subject of a high-resolution multi-proxy investigation which attempted to decipher the impact of some of these dramatic shifts in climate over the later part of the Last Glacial (Wohlfarth *et al.*, 2008). This study found distinct changes in lake productivity which resembled Greenland interstadial–stadial variability. Despite the breadth of palaeoproxies used, some outstanding questions remained relating to hydrological and sedimentological changes within the catchment (Veres *et al.*, 2009).

These types of questions are readily answered through chemical proxies. The chemical record in lake sediments is the integrated result of a variety of factors and processes including source rock composition, catchment weathering, atmospheric deposition, transport efficiencies, sedimentation and post-depositional processes (Boyle, 2002). Past changes in climate will have affected these processes as well as the overall status of the lake in terms of its hydrological regime, internal processes, productivity, etc. How these changes manifest themselves spatially in the sediment record varies and depends partly on the duration of the event *vis-à-vis* sedimentation rates; some events are recorded at sub-millimetre scales, while others are clearly visible in the sediment. Small-scale changes may be missed or their signals diluted when using traditional subsampling and chemical analysis methods.

During the last decade X-ray fluorescence (XRF) core scanning technologies have developed and with such systems it is possible to make high-resolution, non-destructive, *in situ* XRF measurements at sub-millimetre scales (Croudace *et al.*, 2006; Francus *et al.*, 2009), meaning that even the shortest of events can be captured. Such micro-XRF core scanning has successfully been applied to lacustrine sediment sequences to reconstruct, for example, environmental forcings and changes occurring in a 14 ka long sequence from Chile (Moreno *et al.*, 2007; Giralt *et al.*, 2008); variations in aeolian inputs linked to the East Asian monsoon over the last 16 ka (Yancheva *et al.*, 2007); palaeoflood events over the last 2 ka in Spain (Moreno *et al.*, 2008); and changes in sediment input linked to movement of the Intertropical Convergence Zone over the last 55 ka in tropical Africa (Brown *et al.*, 2007). Given the newness of this technology however, the full potential of this

*Correspondence: M. E. Kylander, as above.
E-mail: malin.kylander@geo.su.se

technique has not yet been fully explored. What new information do we gain from such high-resolution elemental analyses? How do these data compare to more traditional palaeoclimate proxies? How can we best use this technique to our advantage?

We broach these topics using the Les Echets sediment sequence which covers a period of known abrupt climate shifts and for which a comprehensive suite of biological, physical and chemical palaeoproxies already exists. The aim of this work is first and foremost to examine the elemental variations that occurred at this site over the last 40 ka as a response to these changes, particular focus on the hydrological regime of the catchment. The specific objectives are to (i) investigate the elemental relationships between Ti, Rb, K, Zr, Si, Ca, Sr, Mn and Fe and how these change over time in the record; (ii) reconstruct shifts in sediment input, grain size and lake levels using chemical proxies; (iii) relate these shifts to the suite of available proxies; and (iv) finally, discuss the wider climatic implications of the elemental data and what it offers.

Materials and methods

Sampling site

Les Echets is located in eastern France, approximately 15 km northeast of Lyon on the Dombes Plateau (45° 54′ N, 4° 56′ E) at 267 m above sea level (Fig. 1). The plateau is covered by glacial deposits, which are assigned to the penultimate glaciation. The Alpine Rhône glacier did not override the Dombes Plateau during the last glaciation but terminated in the valley ~15 km to the east of Les Echets. LGM terminal moraines occur east of the plateau, while associated glaciofluvial deposits are evident further south. The lake basin occupies a depression formed by the Rhône glacier during the penultimate glaciation and is dammed by frontal moraines at its western rim. During the penultimate deglaciation the depression became filled with water; the lake and its sediments thus record environmental change throughout the Last Interglacial/Glacial cycle. At its maximum the lake covered ~1300 ha, but has been filled in gradually starting from the end of the Last Glacial period up to the early Holocene (de Beaulieu and Reille, 1984).

Here we present data from the top 30 m of core EC1, which was retrieved from the central part of the former basin in 2001. The lithostratigraphic Units H to B, as defined previously by Veres *et al.* (2007), will be used to discuss the changes in elemental chemistry occurring in the sediment sequence. These are summarised briefly in Table 1 and delineated in Figs. 2–5.

XRF core scanning

All cores were scanned at the Core Processing Laboratory at the Department of Geological Sciences at Stockholm University using an Itrax XRF core scanner from Cox Analytical Systems (Gothenburg, Sweden). An Itrax scan produces an optical RBG digital image, a microradiographic digital image as well as micro-XRF elemental profiles with an elemental range from Al to U. The generated digital images can be overlaid and compared to changes in elemental composition. For more technical information on the Itrax the reader is referred to Croudace *et al.* (2006).

XRF scans were made using a molybdenum tube set at 30 kV and 25 mA with a dwell time of 30 s. A step size of 1 mm was selected to capture possible elemental variations occurring in laminations observed during logging. The XRF core scans were made on sediments between depths of 3007 and 239 cm, while the original set of palaeoproxies extends between 3007 and 330 cm. Owing to heavy subsampling of the sediment between 2727 and 2403 cm, XRF core scanning data are not available for these depths. Conventional XRF data as an alternative to measure split samples would not have been comparable to the XRF core scanning data presented here. During data reduction the artefacts generated by gaps in other heavily subsampled areas were removed. The data were reduced by averaging to 1 cm intervals and then smoothed using a 10-point running mean. Reproducibility was estimated through repeat spot measurements using a 30 s dwell time with individual relative standard precision (2σ, $n = 54$) of 13% Si, 6% K, 4% Ca, 8% Ti, 18% Mn, 4% Fe, 12% Rb, 9% Sr and 9% Zr. The elemental data presented here have been normalised by incoherent and coherent scattering to account for changes in the water content and density of the sediments during analysis and by several instrumental parameters.

Age model and available palaeoproxies

The age model for the EC1 core is based on 48 accelerator mass spectrometric ^{14}C measurements on plant macrofossils, pollen concentrates and samples of the insoluble bulk sediment

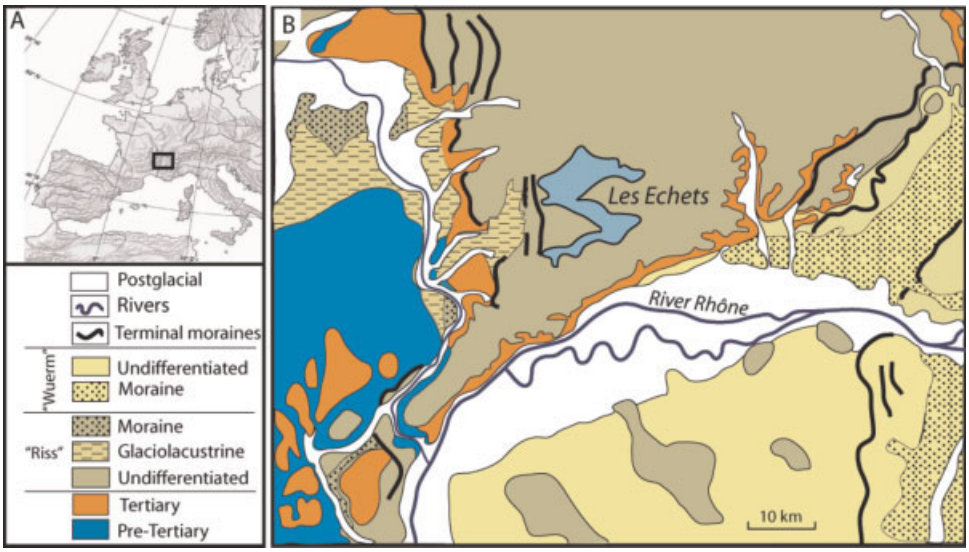

Figure 1. Location of Les Echets in Europe (A) and simplified geological map (B) of the Les Echets palaeolake and environs, modified after Mandier (1981).

Table 1. Correlation matrices (*r* values) for the Les Echets sequence by lithostratigraphic unit.

Unit		K	Ca	Ti	Mn	Fe	Rb	Sr	Zr
H	Si	0.27	0.24	0.41	−0.34	−0.50	0.24	0.87*	0.70*
Clayey gyttja silt,	K		0.01	0.84*	−0.19	−0.12	0.74*	0.19	−0.04
laminated clayey	Ca			−0.24	0.34	0.00	−0.33	0.50	0.41
silt gyttja and	Ti				−0.39	−0.25	0.86*	0.27	−0.03
centimetre-thick	Mn					0.89*	−0.59	−0.40	−0.34
silt and sand	Fe						−0.42	−0.63	−0.61
horizons	Rb							0.17	−0.05
	Sr								0.79*
G	Si	0.80*	−0.53	0.94*	−0.62	−0.19	0.79*	0.44	0.42
Alternating layers of algae	K		−0.38	0.91*	−0.30	0.07	0.78*	0.36	0.05
gyttja rich in OM (>20%)	Ca			−0.60	0.20	0.30	−0.20	0.00	−0.20
and dark-grey clayey	Ti				−0.55	−0.21	0.84*	0.48	0.36
gyttja silt with lower	Mn					0.79*	−0.75*	−0.85*	−0.86*
OM (5–7%). Occasional	Fe						−0.42	−0.75*	−0.82*
lamination and thin	Rb							0.83*	0.60
layers of silt	Sr								0.81*
F	Si	0.11	−0.07	0.21	−0.93*	−0.67	−0.64	0.15	0.49
Clayey gyttja silt	K		−0.47	0.80*	−0.04	0.34	0.60	−0.37	−0.35
alternating with clayey	Ca			−0.68	0.07	−0.24	−0.07	0.58	0.20
silt gyttja, OM content	Ti				−0.15	0.22	0.37	−0.27	0.01
6–12%	Mn					0.76*	0.66	−0.18	−0.49
	Fe						0.68	−0.56	−0.72*
	Rb							−0.21	−0.48
	Sr								0.68
E	Si	0.74*	−0.04	0.64	0.59	0.20	0.55	0.77*	0.60
A massive, faintly	K		−0.57	0.95*	0.42	0.42	0.90*	0.55	0.76*
laminated clayey silt	Ca			−0.65	0.13	−0.42	−0.55	0.17	−0.46
gyttja with OM ∼8%	Ti				0.38	0.44	0.91*	0.49	0.78*
	Mn					0.62	0.16	0.33	0.06
	Fe						0.23	−0.30	0.07
	Rb							0.55	0.81*
	Sr								0.63
D	Si	0.44	−0.39	0.47	−0.12	−0.05	0.26	0.11	0.54
Faintly laminated	K		−0.61	0.96*	0.16	0.51	0.94*	0.23	0.07
clayey gyttja silt with	Ca			−0.71*	−0.01	−0.46	−0.64	0.31	−0.40
low OM (6%).	Ti				0.17	0.49	0.94*	0.25	0.26
	Mn					0.75*	0.06	−0.14	−0.25
	Fe						0.42	−0.36	−0.29
	Rb							0.34	0.14
	Sr								0.25
C	Si	0.40	−0.02	0.31	−0.23	−0.10	0.28	0.30	0.56
A more massive and	K		−0.64	0.95*	−0.28	0.30	0.84*	−0.36	0.47
homogeneous clayey	Ca			−0.78*	0.44	−0.26	−0.75*	0.82*	−0.39
gyttja silt with fewer	Ti				−0.40	0.24	0.91*	−0.48	0.54
laminations than unit D	Mn					0.59	−0.46	0.12	−0.58
	Fe						0.10	−0.53	−0.34
	Rb							−0.38	0.63
	Sr								0.10
B	Si	0.50	−0.60	0.51	−0.45	0.26	0.49	−0.42	0.38
Clayey gyttja silt with	K		−0.79*	0.86*	−0.10	0.78*	0.80*	−0.73*	0.01
frequent calcareous sandy	Ca			−0.92*	0.31	−0.71*	−0.94*	0.93*	−0.40
layers, thin organic layers,	Ti				−0.33	0.71*	0.92*	−0.88*	0.44
sands and faintly laminated	Mn					0.12	−0.32	0.13	−0.52
silty clay, OM 2–10%.	Fe						0.66	−0.77*	0.01
	Rb							−0.92*	0.39
	Sr								−0.39

* Strong correlations ($r \geq 0.7$ or $r \leq -0.7$).

fraction together with 21 infrared stimulated luminescence dates between 3007 and 549 cm. The data presented in this paper, between the depths of 3007 and 239 cm, correspond to an age range from 46.1 to <15.1 ka. For full details of the dates and age model construction the reader is directed to Wohlfarth *et al.* (2008). Analytical details pertaining to those proxies selected for comparison against the new elemental data, namely grain size, total organic carbon (TOC), biogenic silica (BSi) and relative abundance of planktonic and benthic diatom taxa, are available from the original manuscripts (Veres *et al.*, 2007, 2009; Ampel *et al.*, 2008, 2010; Wohlfarth *et al.*, 2008). We also use calcium carbonate ($CaCO_3$) data, which to date is

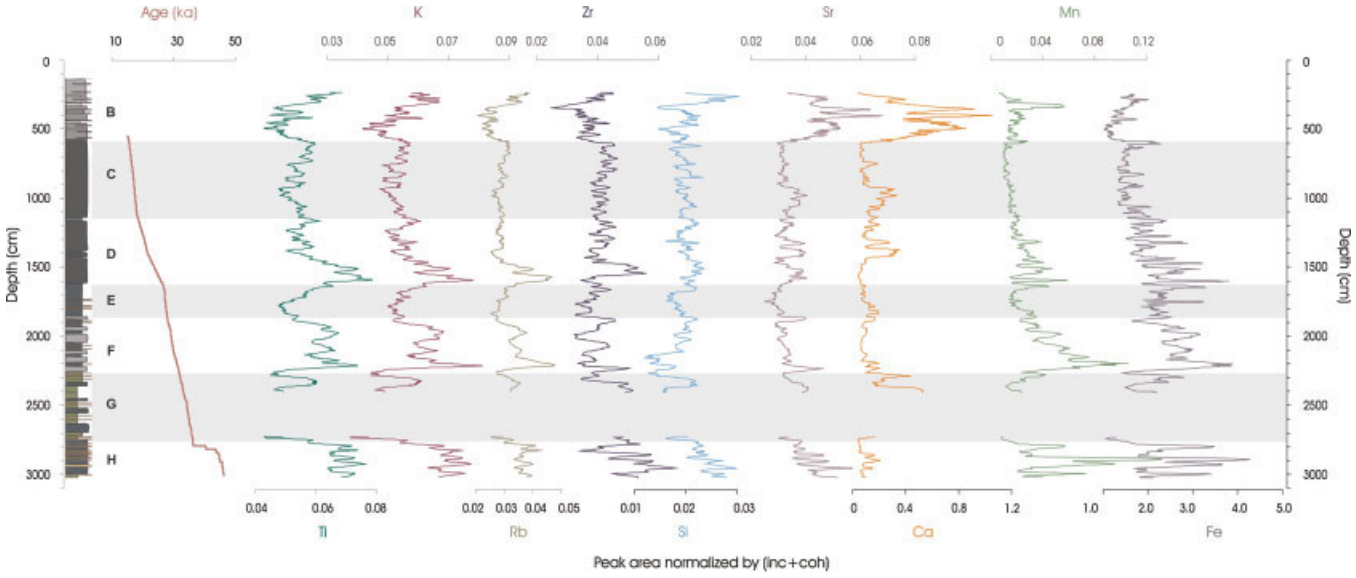

Figure 2. Peak area vs. depth profiles of the elements selected for study. Boundaries of lithostratigraphic Units B to H are shown as well. It was not possible to acquire data between 2727 and 2403 cm. This figure is available in colour online at wileyonlinelibrary.com.

not published. $CaCO_3$ was determined by taking the difference in percentage loss of organic material between sediment combustion at 550 and 925°C and multiplying it by a factor of 2.27 (Dean and Gorham, 1976).

Results and discussion

Correlation matrices: elemental data

The Itrax produces elemental data in terms of peak areas. In a palaeoclimatic context it is the relative changes in the elemental profiles, rather than the absolute concentrations, which are of interest. The peak area vs. depth profiles of those elements selected for study, namely Ti, K, Rb, Zr, Si, Sr, Ca, Mn and Fe, are shown in Fig. 2. Correlation matrices were constructed in order to quantify the strength of association between pairs of elements in the dataset. Changes in the lake lithostratigraphy evidence considerable variation in lake status over time, so a separate correlation matrix was constructed for each unit. In Table 1, strong correlations ($r \geq 0.7$ or $r \leq -0.7$) are highlighted with asterisks.

The constructed correlation matrices show that there is a coupling and decoupling of elements along the length of the profile. The only group of elements that correlate strongly in all

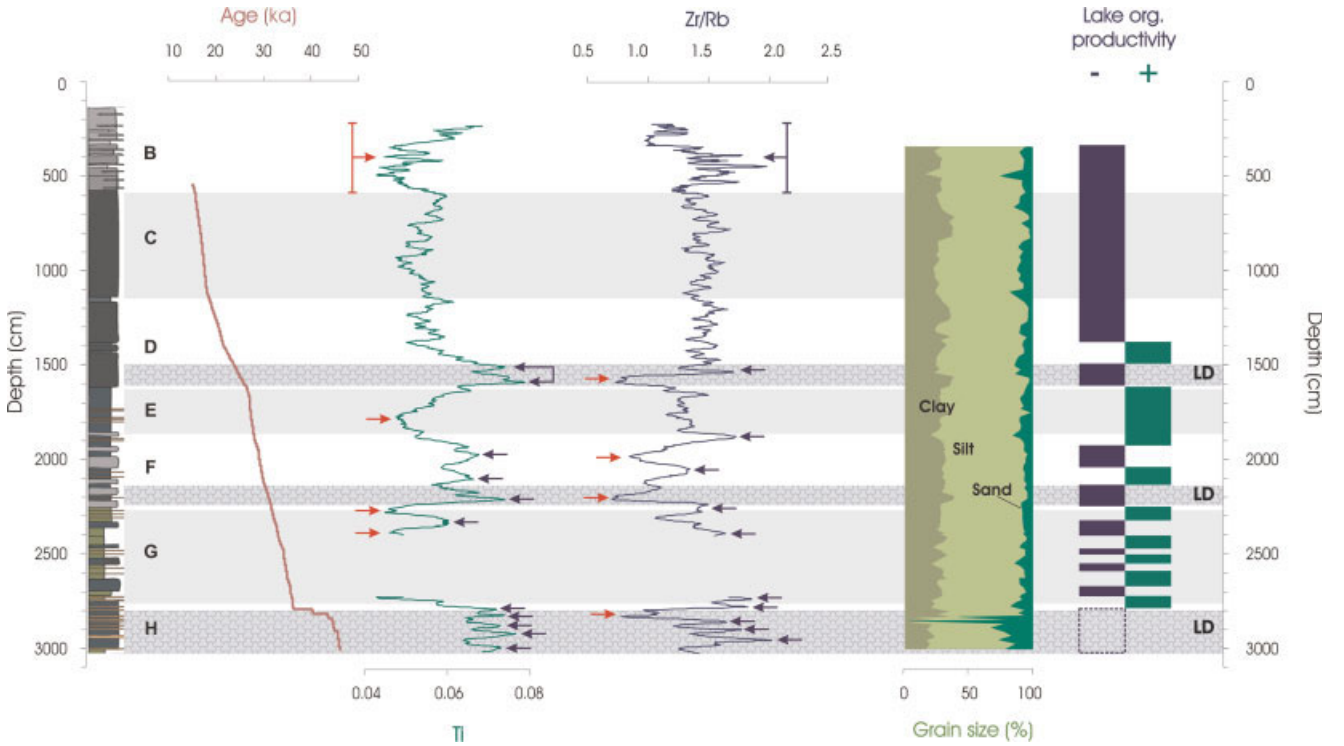

Figure 3. Titanium peak areas and Zr/Rb ratios vs. depth profiles as well as grain size changes and lake productivity shifts established by Wohlfarth *et al.* (2008). Boundaries of lithostratigraphic Units B to H as well as and periods of low diatom (LD) concentrations as established by Ampel *et al.* (2008) are shown. No elemental data exist between 2727 and 2403 cm. Arrows indicate those depths highlighted in the text. This figure is available in colour online at wileyonlinelibrary.com.

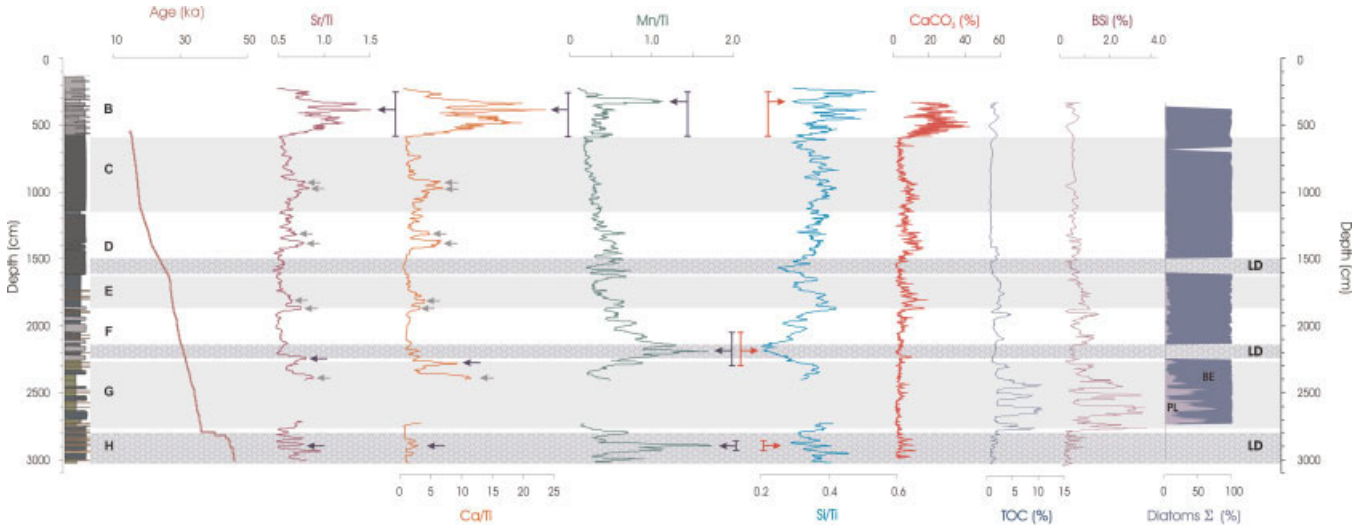

Figure 4. Sr/Ti, Ca/Ti, Si/Ti and Mn/Ti ratios vs. depth profiles as well as $CaCO_3$, TOC, BSi and the relative abundance between planktonic (PL) and benthic (BE) diatom species. Boundaries of lithostratigraphic Units B to H and periods of low diatom (LD) concentrations as established by Ampel *et al.* (2008) are shown. No elemental data exist between 2727 and 2403 cm. Arrows indicate those depths highlighted in the text. This figure is available in colour online at wileyonlinelibrary.com.

units are Ti, Rb and K, which suggests an association with clay minerals and detrital input. Several elements play multiple roles within the system depending on their individual chemistry and on variations in lake status. For example, Si is abundant in many aluminosilicate minerals, particularly alkali feldspars, but is also associated with diatom productivity as a component in their frustules (Peinerud, 2000). Based on good correlations with K, Ti and Rb, Si behaviour is mainly controlled by silicate sources in Unit G. This is not the case elsewhere in the profile, where elemental correlations suggest a combination of minerogenic and biogenic sources of Si. Changes in Fe can be indicative of redox conditions in the lake or of detrital inputs and/or changes in sediment source (Davison, 1993). In Units C to H there is a moderate to strong relationship between Mn and Fe, suggesting control by redox processes. In Unit B, however, Fe is more closely associated with K, Ti and Rb and hence detrital input. Calcium has both allogenic (erosion) and authigenic (within lake precipitation) sources (Cohen, 2003). The strong correlation between Ca and Sr in Units B and C suggests that carbonate precipitation is particularly important late in the record, while in other units (G, E, D), little or no correlation between these two elements exists. Strontium itself can also be associated with silicates, particularly plagioclase feldspars, as in Unit E where it strongly correlates with Ti, Rb, K, Si and Zr. In Unit B a mirroring effect is observed between Ti, K, Rb, (Zr) and (Fe) and Ca and Sr (Fig. 2); these two groups are clearly negatively correlated. It is possible that in this upper unit we are seeing dilution of the elemental signal by carbonates (discussed below) rather than a real change in concentrations in the sediment. Silicon and Mn do not reflect this dilution,

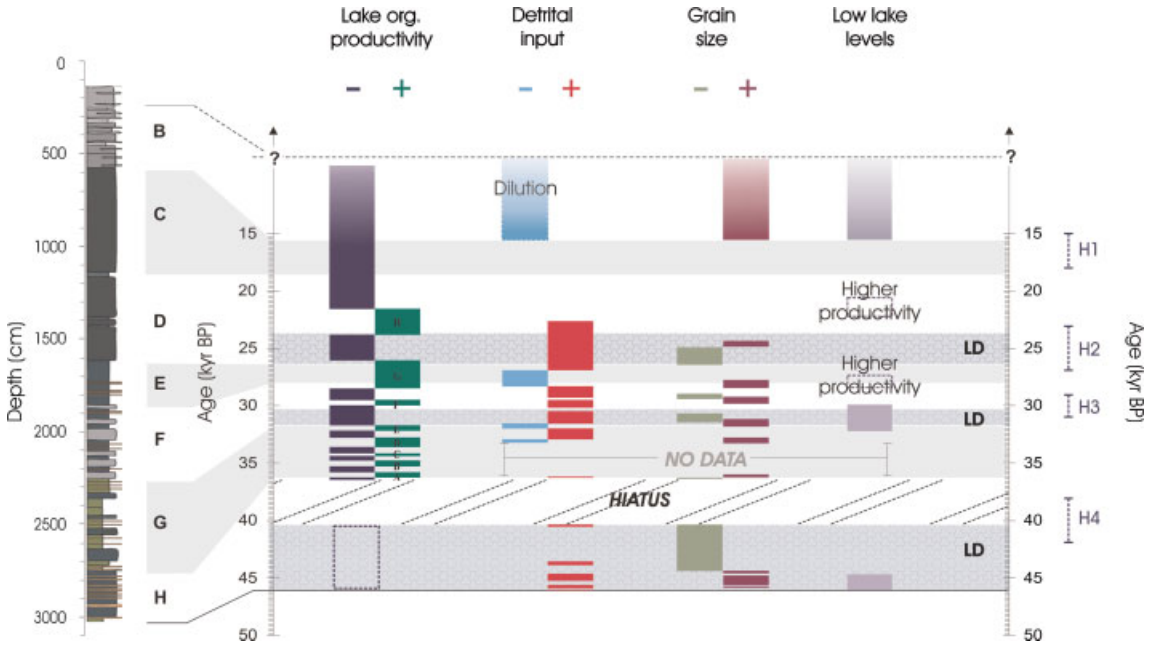

Figure 5. A summary of lake productivity as established by Wohlfarth *et al.* (2008) as well as significant shifts in detrital inputs (based on Ti data), grain size (based on Zr/Rb) and lake levels (based on Sr, Ca and Mn data) plotted as a function of time. Boundaries of lithostratigraphic Units B to H and periods of low diatom (LD) concentrations as established by Ampel *et al.* (2008) are shown. Additionally, published ranges for H4–H1 are shown (see text for references). This figure is available in colour online at wileyonlinelibrary.com.

perhaps due to the influence of diatom productivity/preservation and redox remobilisation, respectively.

The coupling and decoupling of elements evidenced here reflects the history of the lake and changes in its palaeoenvironment. Reconstructions based on the elemental data must consider the fact that the lake history is variable enough for elements to take on different roles at different times, with the main exceptions of Ti, Rb and K. Titanium is used here to normalise the data due to its abundance, conservative nature during transport and weathering, and the fact that it is not biologically important. To avoid artefacts generated by possible dilution (e.g. carbonates, organic matter) (Löwemark *et al.*, 2010) in the discussion that follows, we try to focus mainly on elemental ratios. Nonetheless, TOC values are no greater than 7.3% in the studied sediments. This dilution factor is thus less important and we have confidence in the fact that changes in the single-element profiles are real.

Changes in hydrological regime

The new elemental data allow us to reconstruct changes in the hydrological regime of the catchment as expressed through changes in sediment inputs, grain size and lake levels. One difficulty in interpreting the long elemental record, however, is the fact that there is no clear baseline from which to assess deviations. As such, we highlight extremes in the profile which are interpreted to reflect a relatively significant shift in behaviour.

Detrital inputs: Ti, K, Rb, Zr and Si

Titanium, K, Rb, Zr and Si are all indicative of minerogenic input to the lake. At Les Echets these elements generally show the same trends across the suite with some leads and lags between Ti, K and Rb and Zr and Si (Fig. 2). As suggested by previous studies, the chemistry of sediments is strongly controlled by the grain size of the dominant mineral host and subsequent particle size sorting (e.g. Das and Haake, 2003; Koinig *et al.*, 2003; Jin *et al.*, 2006). Titanium, Rb and K are often associated with clay mineral assemblages, while Zr and Si are generally linked to coarser silt and sand size fractions. Silicon is unique among this group in that it can be biological in source as well, which explains its diverging behaviour in several parts of the profile.

In Unit H shifts in these two groupings are out of phase with each other. Titanium, K and to a lesser extent Rb peak areas are all relatively high in Unit H, with peaks centred on 46.1 ka (2995 cm), 45.7 ka (2928 cm), 44.9 ka (2886 cm), 43.7 ka (2830 cm) and 40.3 ka (2795 cm). Zirconium and Si have peaks centred on 45.8 ka (2952 cm), 44.6 ka (2859 cm) and 36.3 ka (2777 cm). In Units G and F several distinct increases and decreases in the minerogenic elements occur, although the suite is again not entirely cohesive in its behaviour. Specifically, increases in Ti, K and Rb are dated to 33.0 ka (2391 cm); Ti, K, Rb, Zr and Si are dated to 32.7 ka (2350 cm); in Ti, K, Rb, Zr (leading slightly) and Si to 31.3 ka (2214 cm); in Ti, K, Rb and (Si) to 29.9 ka (2106 cm); in Zr at 29.7 ka (2079 cm); in Ti, K and Rb at 29.1 ka (1977 cm); and in Zr and Si to 28.1 ka (1890 cm). A decrease in Ti, K and Rb peak areas straddles the transition between Units G and F (31.9 ka or 2277 cm). A general decrease in these elements is observed in Unit E, most clearly seen in the Ti profile, where it shows a more defined dip between 27.4 ka (1900 cm) and 28.2 ka (1777 cm) with minimum peak areas at 27.5 ka (1788 cm). The most striking feature of the elemental profiles is the simultaneous increase in Ti, K and Rb peak areas occurring in Unit D with maxima at 25.6 ka (1583 cm), while Zr lags slightly, peaking at 24.8 ka (1550 cm). This is followed by a secondary peak at 24.1 ka (1516 cm) in all of the detrital elements. Titanium, K, Rb, Zr and Si show high-frequency, relatively low-amplitude shifts between 21.6 and 15.6 ka (1399–591 cm), with larger-amplitude shifts in Ti, K and Zr occurring from 17.4 ka (954 cm) up to 15.1 ka at the boundary between Unit C and B (591 cm). Unit B is significant in its decrease in measured peak areas of minerogenic elements which, as mentioned previously, is likely a result of carbonate dilution.

It is clear that there are variations in the amounts and character of the detrital material entering the lake. The nature of these additions is, however, unclear from the elemental changes discussed above; are these changes driven by increased hydrological activity or are we seeing signals of a more arid climate?

Grain size changes: Zr/Rb

The behaviour of Rb and Zr can be exploited to acquire information on grain size and sediment composition. Rubidium is present in several common minerals including mica and clay minerals, and displays low environmental mobility mainly due to its very strong sorption to clay minerals, particularly at high pH. Its ability to substitute for K in the crystal lattice, however, means that it can also be found in K-feldspar. Zirconium is normally enriched in medium to coarse silts and is associated with heavy minerals like zircon. In finer-grained sediments Zr/Rb can be used as a proxy for changes in grain size, with lower values representing fine-grained material and higher values representing coarse-grained material (Dypvik and Harris, 2001). This relationship does not hold, however, if there is a significant contribution of Rb from K-feldspars, which are commonly associated with coarse silt and sand size fractions. Examination of the relationship of Ti, which is representative of fine size fractions, with K and Rb gives correlations with high r values of 0.92 and 0.86, respectively, suggesting that coarser grain sizes are not important hosts for K or Rb. Grain size analyses from Wohlfarth *et al.* (2008) show that with the exception of Unit H sands account for on average 7% of the sediment. Investigation of how the individual grain size fractions in each unit correlate to the elemental data (data not shown) demonstrates that where correlations do exist Ti, K and Rb are associated with clays, very fine silts and fine silts (Units B and F), while Zr is associated with very find sands and fine sands (Unit D). It is thus reasonable to interpret changes in Zr/Rb as a proxy for major grain size changes.

Figure 3 plots Ti (with peaks discussed in the text highlighted), included here as a proxy for (fine) detrital inputs and Zr/Rb ratios as a proxy for grain size changes. To validate the interpretation of the elemental ratios, we use proxy data from the original high-resolution dataset in the form of grain size analysis and lake productivity shifts as reconstructed based on a variety of proxies by Wohlfarth *et al.* (2008). Highlighted also are three periods of low diatom concentration (LD) (Ampel *et al.*, 2008).

Based on the Zr/Rb proxy, large shifts in grain size occur within Unit H, with increases in Zr/Rb occurring at 45.9 ka (2954 cm), 45.0 ka (2897 cm), 44.6 ka (2863 cm), 36.3 ka (2777 cm) and 36.1 ka (2737 cm). Indeed, each of these increases is matched by an increase in the sand fraction as evidenced by the grain size analysis. A decrease in the Zr/Rb ratio occurs at 43.8 ka (2830 cm) which is matched by an increase in clay and sand fractions. Further on in the profile increases in Zr/Rb occur at 33.0 ka (2394 cm), 31.7 ka (2250 cm), 29.7 ka (2072 cm), 28.1 ka (1890 cm), 24.7 ka (1545 cm) and from 15.1 ka in Unit B (from 591 cm). Decreases in this same ratio occur at 31.2 ka (2208 cm), 29.0 ka (1990 cm) and 25.8 ka (1596 cm) (Fig. 3). In general, increases in the Zr/Rb

ratio are associated with increases in the coarse size fractions, while decreases coincide with increases in the clay fraction. This confirms the control that grain size has on the elemental variations found in the sediment record at Les Echets. The surprisingly low mathematical correlation between the grain size and elemental data, given the visual agreement described above, is likely a result of differences in sampling resolution (2 cm for grain size and 1 cm averaged for the Itrax data) and matching of the profiles.

Lake levels and productivity: Ca, Sr, Mn and Si

Calcium and Sr in lake sediments are related to carbonate weathering in the catchment and in-lake precipitation of $CaCO_3$ with co-precipitation of $SrCO_3$. The latter occurs when the chemical concentration of lake waters reaches the point of carbonate saturation, as when lake waters are concentrated by a lowering of lake levels (Cohen, 2003). Figure 4 shows the Ti normalised profiles of Sr, Ca, Si and Mn as well as the related proxies of $CaCO_3$, TOC, BSi and diatom abundances.

The bedrock of the Dombes Plateau is dominated by limestones and a limestone component is also present in the overlying glaciofluvial and loessic sedimentary deposits, providing a large pool of carbonates to draw from. Ca/Ti and Sr/Ti are well correlated throughout the entire profile, with an r value of 0.94. This strong association is driven mostly by the topmost Units B and C where, as confirmed by the $CaCO_3$ curve in Fig. 4, carbonate precipitation is important. Table 1 shows in fact that Units G, E and D have lower correlations between Ca and Sr, where the latter acts more like the allochotonous elements Ti, Rb, K, Zr and Si.

Manganese forms a highly insoluble oxide in an oxygen-rich environment and migrates up to the oxic boundary. Changes in lake oxygen levels can be the result of changes in lake levels and ventilation of the water column or increased biological activity (photosynthesis) by limnic organisms (Davidson, 1993). The largest peaks in Mn/Ti are dated to 44.9 ka (2894 cm), 32.1 and 29.5 ka (2304–2049 cm) and <15.1 ka (Unit B, main peak at 342 cm) (Fig. 4). These Mn/Ti peaks are associated with decreases in Si/Ti, reflecting changes in biological activity, and suggest that increased photosynthesis cannot explain the Mn/Ti peaks. Rather, Mn precipitation must be a sign of oxygenation of the bottom waters through lowering of lake levels as seen, for example, in the Lago Chungará sequence (Moreno *et al.*, 2007). This is further supported by moderate peaks in Ca/Ti and Sr/Ti. Indeed, the correlation between Ca/Ti (representing the carbonates) and Si/Ti (representing diatoms) is low in Units F (0.12) and B (0.08), suggesting that productivity blooms are not the main promoter of carbonate production. These interpretations are corroborated by TOC, BSi and diatom concentrations, where the most significant peaks in Mn/Ti are matched by decreases in these proxies and hence lake productivity.

Secondary Mn/Ti peaks are associated with peaks in Sr/Ti and Ca/Ti at 33.0 ka (2391 cm), 28.0 ka (1886 cm), 27.4 ka (1775 cm), 21.6 ka (1400 cm), 20.8 ka (1326 cm) and 17.5 ka (983 and 973 cm) (Fig. 4). The group of peaks occurring in Units D and E and parts of Unit F are associated with increases in Si/Ti which would evoke the occurrence of an algae bloom and not necessarily a lowering of lake levels; indeed, BSi curves show peaks at these depths as well.

Climatic Implications

The elemental data have reconstructed a history of changes in sediment inputs, grain size, lake productivity and lake levels. We summarise this information in Fig. 5, where the highlighted peaks shown in Figs. 3 and 4 and discussed in the text are plotted on an age scale. Also given are the lake productivity shifts as established by Wohlfarth *et al.* (2008) and Veres *et al.* (2009), the lithostratigraphic boundaries as defined by Veres *et al.* (2007) and periods with low diatom concentrations (LD) as identified by Ampel *et al.* (2008). In addition, published age ranges for H4 to H1 have been included (Combourieu Nebout *et al.*, 2002, 2009; Sánchez Goñi *et al.*, 2002; Roucoux *et al.*, 2005; Rousseau *et al.*, 2007; Fletcher and Sánchez Goñi, 2008).

Recorded impacts from climate change events

The suite of proxies used by Wohlfarth *et al.* (2008) identified the response of lake productivity at Les Echets to established climate oscillations, namely the Greenland stadials–interstadials 8–2 and H4–H2 events. It appears that the elemental data have also captured some of these events. Several of the highlighted periods of lower detrital input (decreased Ti) and additions of coarser-grained material (increased Zr/Rb) are coincident with previously defined periods of higher lake productivity, namely lake productivity periods D, E and G (Fig. 5).

Unit H, dating to between 46.1 and 36.2 ka, is characterised by low diatom concentrations and the deposition of alternating layers of silt and sand. Its most significant feature is a hiatus occurring between 40.3 and 36.3 ka. The signals archived in this unit have been difficult to interpret based on previous proxy data but Unit H does partly overlap with ages reported for H4 (Combourieu Nebout *et al.*, 2002; de Abreu *et al.*, 2003; Roucoux *et al.*, 2005; Fletcher and Sánchez Goñi, 2008). As H4 was one of the most severe H events (Sánchez Goñi *et al.*, 2002; Vautravers and Shackleton, 2006) it has been suggested that extremely harsh and arid conditions associated with this event might have resulted in low lake levels, an open landscape and exposed shores leading to an unstable depositional environment with high input of coarse sediment and reworking of sediments at Les Echets. It remains unclear in terms of the elemental data if H4 is recorded or if its signal has been disturbed.

Perhaps the most obvious feature of the chemical record is the increase in detrital elements (increases in Ti) and fine-grained (decreases in Zr/Rb) inputs centred on 31.2 ka (2208 cm) and 25.8 ka (1596 cm) (Figs. 3 and 5); the former shift is also associated with low lake levels as established using Ca, Sr and Mn data (Fig. 4). These features are coincident with the presence of very few diatom frustules in the Les Echets record (Figs. 3–5) (Ampel *et al.*, 2008) and overlap in time with published estimates for H3 and H2 in Europe and surrounding regions, respectively (Bard *et al.*, 2000; de Abreu *et al.*, 2003; Roucoux *et al.*, 2005; Fletcher and Sánchez Goñi, 2008; Combourieu Nebout *et al.*, 2009). Indeed H events are known to have been cold and arid with reduced vegetation cover and exposed soils and we would expect such changes to be reflected in our chemical proxies. Grain size changes can provide some indication as to the dominant modes of transport during these palaeoenvironmental shifts, with coarser grain sizes indicative of transport via hydrological pathways and finer grain sizes indicative of aeolian transport, although this interpretation must be made with caution (Last, 2001). Given the plateau location of this site and the presence of easily erodible glaciofluvial and loessic sedimentary material, it can be hypothesised that the fine-grained material deposited at the site during H events is dominantly aeolian in source. This hypothesis is supported by the detailed study of the loess sequence at Nussloch in Germany (Rousseau *et al.*, 2007), which shows distinct changes in aeolian sediment deposition related to wind strength, especially during H3 and H2. Interstadial periods, on the other hand, were associated with palaeosol development, suggesting less windy and moister conditions (Rousseau *et al.*, 2007). Due to the very mixed

nature of the sediments surrounding the site it is not, however, possible to make any source tracing of these sediments to test this hypothesis.

The increased detrital input evidenced during H3 and H2 would decrease light penetration within the water column – an effect which would be enhanced during periods of low lake levels (as during H3) where more mixing of the water column is likely, particularly in an environment with an altered wind regime. Ampel *et al.* (2008) speculated that the dramatic decrease in diatom frustules coinciding with H events was a consequence of either increased dissolution, light deficiency due to higher turbidity and heavy sediment input, extensive ice coverage or a combination of these. The elemental data show that increased sediment input and higher turbidity were, if not the sole factors, at least of significant importance.

None of the lake productivity proxies or diatom assemblage data indicate a distinct change that can be interpreted as a response to the LGM. No clear change in the elemental data can be associated with H1 either, although lower lake levels are reconstructed between 17.5 ka (983 and 973 cm) up to the start of Unit B (591 cm), which overlaps with ages reported for H1 (Bard *et al.*, 2000; Fletcher and Sánchez Goñi, 2008; Combourieu Nebout *et al.*, 2009). On the other hand, it is hard to separate this effect from the infilling of the lake. The chemical analysis of Unit B from 591 to 239 cm (<15.1 ka) suggests wetter conditions but lower lake levels.

Duration of Heinrich event impacts at Les Echets

The different biological, chemical and physical proxies analysed at Les Echets clearly register a response to H events, although the duration and intensity of the impact differ depending on which proxy is selected. On the basis of low diatom concentrations, the impact of H3 would last 1.4 ka (31.7–30.3 ka), while the impact of H2 would span over 2.7 ka (26.3–23.6 ka) (Ampel *et al.*, 2008). If one uses the minerogenic elements to establish the timing and duration of a response to H events, a slightly different picture emerges. Indeed, it is unclear which peak would represent H3 (Figs. 2 and 3). Based on the primary peak in Ti a duration of 300 a (31.4–31.1 ka or 2228–2199 cm) or, when using both peaks, 0.7 ka (31.4–30.7 ka or 2228–2167 cm) can be estimated for H3. In terms of H2, the increase in Ti begins already at ~27 ka and peaks at 25.6 ka (1583 cm), which does not suggest the abrupt change in climate usually associated with H events. Using the main Ti, K and Rb peak, H2 would cover the time period from 26 ka (1605 cm) to 25 ka (1557 cm) or 1 ka. If the response to H3 is estimated based on Zr/Rb, this event covers 0.5 ka and is centred on 31.2 ka (2208 cm). If we estimate the duration of H2 from the twin peaks at 1594 and 1564 cm, it would date to between 25.8 and 25.1 ka or span 0.7 ka with a maximum possible range of 26.3–25 ka or 1.3 ka.

The diatom-based proxies and the chemical proxies are characterised by different sampling resolution with continuous 1 cm averages used for XRF core scanning and 2 cm aliquots on an average spacing of 7 cm for diatom analyses. Over the distinct shifts in diatom abundance associated with H events, however, subsampling was made continuously. Even though a single diatom subsample represents a larger time span (2 cm aliquot) than a single XRF measurement we do not consider the duration of the impact of H events on either proxy to be an artefact of a difference in sample resolution. The changes in diatom abundance occur on a sample-to-sample basis and the changes in XRF data do not coincide with those samples at either the start and end of any identified H event impact.

The estimated duration of H event impacts at Les Echets based on the diatom assemblage data and elemental analyses both fall within the range of durations from other marine and terrestrial records in and around the North Atlantic and Europe. Previously published estimates for the duration of H events includes: ca. 0.5 ka on average for any H event (Hemming, 2004); ca. 2–5 ka for H1; ca 1.0–3.0 ka for H2; ca. 0.5–1.5 for H3; and ca. 1.5–5.0 for H4 (Combourieu Nebout *et al.*, 2002, 2009; Sánchez Goñi *et al.*, 2002; Roucoux *et al.*, 2005; Rousseau *et al.*, 2007; Fletcher and Sánchez Goñi, 2008). This wide range of duration estimates for H event impacts does not lend support for preferentially relying on either diatom-, single element- or elemental ratio-based estimates at Les Echets and demonstrates the difficulty with defining a climate 'event' as different proxies have different responses and response times.

Conclusions

The record from Les Echets shows that significant variations in palaeoclimate occurred during the Last Glacial. High-resolution multi-proxy analyses revealed many of these key changes but the addition of elemental data has provided a better understanding of hydrological changes and changes in sediment influx and character in the catchment. Major findings from this study include the following:

1. The correlation matrices constructed for each lithostratigraphic unit show that there is a coupling and decoupling of association between elemental pairs over the long and variable history of the lake. Many of the elements take on different roles, which in this system are related to sediment input, transport and sorting, catchment weathering, biological productivity, redox and salinity conditions in the lake.
2. The influence of several major climate events (H4–H2) was captured using Ti as a proxy for (fine-grained) detrital input and Zr/Rb as a proxy for grain size changes, while Ca, Sr and Mn were used to decipher lake level and productivity changes.
3. The elemental data were able to provide information that could be linked to a number of proxies (grain size analysis, $CaCO_3$, BSi, magnetic susceptibility, diatom assemblages, TOC) and show that non-destructive, high-resolution XRF core scanning makes an excellent first step in the planning of subsampling campaigns.
4. These data demonstrate the difficulty in defining a climate event when using proxy data. Individual proxies are subject to different thresholds which, as evidenced above, leads to variable estimates in duration, in addition to the uncertainties intrinsic to dating the actual occurrence of the event.

Acknowledgements. M. Kylander and B. Wohlfarth acknowledge the financial support of the Swedish Research Council. This is a contribution to the European Science Foundation EuroCores on EuroCLIMATE project RESOLuTION.

Abbreviations. LGM, Last Glacial Maximum; TOC, total organic carbon; XRF, X-ray fluorescence.

References

Ampel L, Wohlfarth B, Risberg J, *et al.* 2008. Paleolimnological response to millennial and centennial scale climate variability during MIS 3 and 2 as suggested by the diatom record in Les Echets, France. *Quaternary Science Reviews* **27**: 1493–1504.

Ampel L, Wohlfarth B, Risberg J, *et al.* 2010. Diatom assemblage dynamics during abrupt climate change: the response of lacustrine diatoms to Dansgaard–Oeschegr cycles during the last glacial period. *Journal of Paleolimnology* **44**: 397–404.

Bard E, Rostek F, Turon J-L, *et al.* 2000. Hydrological impact of Heinrich events in the subtropical northeast Atlantic. *Science* **289**: 1321–1324.

Bond G, Broecker W, Johnsen S, *et al.* 1993. Correlations between climate records from North Atlantic sediments and Greenland ice. *Nature* **365**: 143–147.

Boyle JF. 2002. Inorganic geochemical methods in paleolimnology. In *Tracking Environmental Change Using Lake Sediments: Physical and Geochemical Methods*, Last WM, Smol JP (Eds). Springer: Berlin; pp. 83–141.

Brown ET, Johnson TC, Scholz CA, *et al.* 2007. Abrupt change in tropical African climate linked to the bipolar seesaw over the past 55,000 years. *Geophysical Research Letters* **34**: L20702.

Clark PU, Dyke AS, Shakun JD, *et al.* 2009. The Last Glacial Maximum. *Science* **325**: 710–714.

Cohen AS. 2003. *Paleolimnology: The History and Evolution of Lake Systems*. Oxford University Press: Oxford.

Combourieu Nebout N, Turon JL, Zahn R, *et al.* 2002. Enhanced aridity and atmospheric high-pressure stability over the western Mediterranean during the North Atlantic cold events of the past50k. y. *Geology* **30**: 863–866.

Combourieu Nebout N, Peyron O, Dormoy I, *et al.* 2009. Rapid climatic variability in the west Mediterranean during the last 25 000 years from high resolution pollen data. *Climate of the Past* **5**: 503–521.

Croudace IW, Rindby A, Rothwell RG. 2006. ITRAX: description and evaluation of a new multi-function X-ray core scanner. In *New Techniques in Sediment Core Analysis*, R. Rothwell G (ed.). Geological Society of London: London; 51–63.

Dansgaard W, Johnsen SJ, Clausen HB, *et al.* 1993. Evidence for general instability of past climate from a 250-kyr ice-core record. *Nature* **364**: 218–220.

Das BK, Haake B-G. 2003. Geochemistry of Rewalsar Lake sediment, Lesser Himalaya, India: implications for source-area weathering, provenance and tectonic setting. *Geoscience Journal* **7**: 299–312.

Davison W. 1993. Iron and manganese in lakes. *Earth-Science Reviews* **34**: 119–163.

de Abreu L, Shackleton NJ, Schönfeld J, *et al.* 2003. Millennial-scale oceanic climate variability off the Western Iberian margin during the last two glacial periods. *Marine Geology* **196**: 1–20.

de Beaulieu JL, Reille M. 1984. A long Upper Pleistocene pollen record from Les Echets, near Lyon, France. *Boreas* **13**: 111–132.

Dean WE, Gorham E. 1976. Major chemical and mineral components of profundal surface sediments in Minnesota lakes. *Limnology and Oceanography* **21**: 259–284.

Dypvik H, Harris NB. 2001. Geochemical facies analysis of fine-grained siliciclastics using Th/U, Zr/Rb and (Zr+Rb)/Sr ratios. *Chemical Geology* **181**: 131–146.

Fletcher WJ, Sánchez Goñi MF. 2008. Orbital- and sub-orbital-scale climate impacts on vegetation of the western Mediterranean basin over the last 48,000 yr. *Quaternary Research* **70**: 451–464.

Francus P, Lamb H, Nakasawa T, *et al.* 2009. The potential of high-resolution X-ray fluorescence core scanning: applications in paleolimnology. *PAGES News* **17**: 93–95.

Giralt S, Moreno A, Valero-Garcés B, *et al.* 2008. A statistical approach to disentangle environmental forcings in a lacustrine record: the Lago Chungará case (Chilean Altiplano). *Journal of Paleolimnology* **40**: 195–215.

Hemming SR. 2004. Heinrich events: massive late Pleistocene detritus layers of the North Atlantic and their global climate imprint. *Reviews of Geophysics* **42**: RG10.

Jin ZD, Li FC, Cao JJ, *et al.* 2006. Geochemistry of Daihai Lake sediments, Inner Mongolia, north China: implications for provenance, sedimentary sorting, and catchment weathering. *Geomorphology* **80**: 147–163.

Johnsen SJ, Clausen HB, Dansgaard W, *et al.* 1992. Irregular glacial interstadials recorded in a new Greenland ice core. *Nature* **359**: 311–313.

Koinig KA, Shotyk W, Lotter AF, *et al.* 2003. 9000 years of geochemical evolution of lithogenic major and trace elements in the sediment of an alpine lake: the role of climate, vegetation, and land-use history. *Journal of Paleolimnology* **30**: 307–320.

Last WM. 2001. Textural analysis of sediments. In *Tracking Environmental Change Using Lake Sediments: Physical and Chemical Techniques*, Last WM, Smol J (eds). Kluwer Academic: Dordrecht; 41–81.

Lowe JJ, Rasmussen SO, Björck S, *et al.* 2008. Synchronisation of palaeoenvironmental events in the North Atlantic region during the Last Termination: a revised protocol recommended by the INTIMATE group. *Quaternary Science Reviews* **27**: 6–17.

Löwemark L, Chen H-F, Yang T-N, *et al.* 2010. Normalizing XRF-scanner data: a cautionary note on the interpretation of high-resolution records from organic-rich lakes. *Journal of Asian Earth Sciences* (in press).

Mandier P. 1981. Le marais des Echets: premiers enseignments pour l'histoire clamato-stratigraphique du Quartenaire Lyonnais. *Bulletin du Labratoire Rhodanien de Geomorphologie* **99**: 39–61.

Moreno A, Giralt S, Valero-Garcés B, *et al.* 2007. A 14 kyr record of the tropical Andes: the Lago Chungará sequence (18° S, northern Chilean Altiplano). *Quaternary International* **161**: 4–21.

Moreno A, Valero-Garcés B, González-Sampériz P, *et al.* 2008. Flood response to rainfall variability during the last 2000 years inferred from the Taraville Lake record (central Iberian Range, Spain). *Journal of Paleolimnology* **40**: 943–961.

Peinerud EK. 2000. Interpretation of Si concentrations in lake sediments: three case studies. *Environmental Geology* **40**: 64–72.

Roucoux KH, de Abreu L, Shackleton NJ, *et al.* 2005. The response of NW Iberian vegetation to North Atlantic climate oscillations during the last 65 kyr. *Quaternary Science Reviews* **24**: 1637–1653.

Rousseau D-D, Sima A, Antoine P, *et al.* 2007. Link between European and North Atlantic abrupt climate changes over the last glaciation. *Geophysical Research Letters* **34**: L22713.

Sánchez Goñi MF, Cacho I, Turon J-L, *et al.* 2002. Synchroneity between marine and terrestrial responses to millennial scale climatic variability during the last glacial period in the Mediterranean region. *Climate Dynamics* **19**: 95–105.

Sánchez Goñi MF, Landais A, Fletcher WJ, *et al.* 2008. Contrasting impacts of Dansgaard–Oeschger events over a western European latitudinal transect modulated by orbital parameters. *Quaternary Science Reviews* **27**: 1136–1151.

Vautravers MJ, Shackleton NJ. 2006. Centennial-scale surface hydrology off Portugal during Marine Isotope Stage 3: insights from planktonic foraminiferal fauna variability. *Paleoceanography* **21**: PA3004.

Veres D, Wohlfarth B, Andrieu-Ponel V, *et al.* 2007. The lithostratigraphy of the Les Echets basin, France: tentative correlation between cores. *Boreas* **36**: 326–340.

Veres D, Lallier-Vergès E, Wohlfarth B, *et al.* 2009. Climate-driven changes in lake conditions during late MIS 3 and MIS 2: a high-resolution geochemical record from Les Echets, France. *Boreas* **38**: 230–243.

Wohlfarth B, Veres D, Ampel L, *et al.* 2008. Rapid ecosystem response to abrupt climate changes during the last glacial period in western Europe, 40-16 ka. *Geology* **36**: 407–410.

Yancheva G, Nowaczyk NR, Mingram J, *et al.* 2007. Influence of the intertropical convergence zone on the East Asian monsoon. *Nature* **445**: 74–77.